# Automatic All Quadrilateral Mesh Adaption through Refinement and Coarsening

Bret D. Anderson[1], Steven E. Benzley[1], and Steven J. Owen[2,⋆]

[1] Brigham Young University, Provo, Utah, USA
bret.d.anderson@gmail.com, seb@et.byu.edu
[2] Sandia National Laboratories, Albuquerque, New Mexico, USA
sjowen@sandia.gov

**Abstract.** This work presents a new approach to conformal all-quadrilateral mesh adaptation. Most current quadrilateral adaptivity techniques rely on mesh refinement or a complete remesh of the domain. In contrast, we introduce a new method that incorporates both conformal refinement and coarsening strategies on an existing mesh of any density or configuration. Given a sizing function, this method modifies the mesh by combining template-based quadrilateral refinement methods with recent developments in localized quadrilateral coarsening and quality improvement into an automated mesh adaptation routine. Implementation details and examples are included.

**Keywords:** quadrilateral, adaptivity, refinement, coarsening.

## 1 Introduction

The ability to automatically adapt a finite element mesh based on a sizing function is an important component of an automatic modeling and simulation process. Although it is not a new concept, its principal application has been to triangle and tetrahedral-based methods. Quadrilateral meshes are often preferred by analysts for improved accuracy over triangle-based methods. In spite of this, adaptive quadrilateral techniques are not as prevalent in the literature.

A truly general mesh adaptation scheme must have the ability to both enhance (refine) and simplify (coarsen) a mesh to provide sufficient accuracy and efficiency in the analysis. While there are numerous methods currently used, relatively few provide for both refinement and coarsening. Additionally, no current algorithm has the ability to adapt an all-quadrilateral mesh with refinement and a coarsening technique not constrained to de-refining.

This work presents a unique all-quadrilateral mesh adaptation algorithm that modifies a given mesh by adding and removing elements and employs a

⋆ Sandia is a multiprogram laboratory operated by Sandia Corporation, a Lockheed Martin Company, for the United States Department of Energys National Nuclear Security Administration under contract DE-AC04-94AL85000.

coarsening process that is not limited to undoing previous steps of refinement. This algorithm combines template-based quadrilateral refinement techniques [1] with recent developments in coarsening [2] and quadrilateral improvement [3] to adapt an existing mesh. Additionally, to provide an algorithm that will meet conformity and element type requirements of finite element solvers, this method guarantees a fully conformal, all-quadrilateral mesh.

## 2 Background

To meet the ever increasing computational demands of complex finite element models, mesh adaptation has become a valuable area of study. There are three basic classes of adaptation, commonly referred to as $r-$, $h-$, and $p-$adaptation. $r-$adaptation, sometimes known as smoothing, refers to methods that alter element geometry by repositioning the nodes, but do not change the topology of the mesh. $h-$adaptation, refers to methods which change both the geometry of the elements and the topology of the mesh by adding and/or removing elements. $p-$adaptation, involves methods that do not alter the geometry or topology of individual elements; instead, these techniques change the degree of the elements in the mesh. While recognizing the importance of both $r-$ and $p-$adaptive methods we focus this work on the $h-$adaptive technique, concentrating specifically on the conformal refinement and coarsening of all-quadrilateral meshes.

### 2.1 Current Methods

Initial adaptive mesh generation is perhaps the easiest way to build an adapted finite element mesh because it simply employs the given sizing function in the original creation of the mesh. This is a widely used method and is available in many mesh generation schemes, including paving [4]. The major drawback of initial adaptive mesh generation is that it requires significant foresight into the probable results of the analysis which are used to determine element sizes and an appropriate distribution of element density across the mesh. Because of this required foresight, initial mesh generation techniques that incorporate sizing are particularly useful when based on geometric characteristics of the model [5].

Closely related to initial adaptive mesh generation is adaptive mesh regeneration; a mesh adaptation scheme in which the mesh is analyzed, a sizing function is determined, and the entire mesh or the region of the mesh requiring modification is removed and reconstructed according to the new sizing function. A significant amount of research has been done in this area and numerous algorithms have been presented employing adaptive mesh regeneration [6] [7] [8]. Although regenerating the mesh does not have the same drawbacks with respect to required foresight as does initial adaptive mesh generation, deleting and re-creating the mesh can be inefficient when only a small region requires adaption. In addition, the initial mesh generation may

specify detailed user controls requiring specific local sizing and quality. Regenerating a complete mesh in these circumstances when only a small portion is required to be adapted may not be a feasible option.

### 2.2 Concurrent Refinement and Coarsening

While there are many effective methods that have been proposed in the literature [9] - [13] to adapt a mesh, none address the ability to provide effectively coupled coarsening and refinement for quadrilateral meshes. Utilization of both coarsening and refinement in mesh adaptation greatly increases the ability to modify a mesh to provide an appropriate element density without the need to know the coarsest state of the model.

Hierarchical adaptation methods [14] have been developed that are able to adapt all-quadrilateral meshes, while maintaining conformity, by using quadtree refinement with transition templates. Coarsening in hierarchical adaptation is accomplished by simply removing quadtrees from parent elements; however, a major limitation of this method is that there is no way for the mesh to be coarsened further than the initial base mesh. By taking advantage of new coarsening techniques the algorithm presented in this work provides adaptation that includes coarsening not limited to undoing previous refinement.

## 3 Automated Mesh Adaptation

### 3.1 Sizing Functions

The first step in creating an adaptive mesh is to provide an appropriate sizing function across the mesh domain. Sizing functions are typically based on error estimates derived from the solution of a finite element analysis, geometric characteristics of the model, or other user defined constraints. A solution based sizing function might specify an increased element density in regions of high stress or strain gradients. Geometry based sizing functions, such as a skeleton sizing function [5] [15], consider feature size as well as surface or boundary curvature and specify an appropriate element density throughout the mesh.

In addition to specifying the desired size of elements throughout the mesh, sizing functions must also take into account mesh gradation, the rate at which the element sizes change across the mesh [16] [17]. Gradation control is an important part of ensuring high shape quality of elements in a conformal mesh by not allowing a large change in size between adjacent elements. Although it is an important area of study, the development of sizing functions is not part of this research and it is assumed that an appropriate sizing function is provided as input to each adaptive meshing problem.

### 3.2 Tools and Requirements

The adaptation technique presented in this work employs a combination of quadrilateral refinement, coarsening, and quality improvement operations to adapt a given mesh. Since some finite element solvers require a conformal mesh and others do not allow hybrid meshes with more than one element type, only adaptation operations that preserve a conformal all-quadrilateral mesh are used. Additionally, these operations must be able to be applied locally to allow for concurrent coarsening and refinement.

Since the primary goal of adaptation is to ensure accurate results, refinement is usually required. This adaptation algorithm employs a refinement method that subdivides faces in the refinement region using a four element quadtree, referred to as 2-refinement, with templates inserted into the transition zone to maintain a conformal all-quadrilateral mesh [18] (see figure 1(b)). While nine element quadtrees or 3-refinement (see figure 1(c)) are sometimes used to refine quadrilateral faces, 2-refinement was chosen because it offers more control over the number of elements added to the mesh.

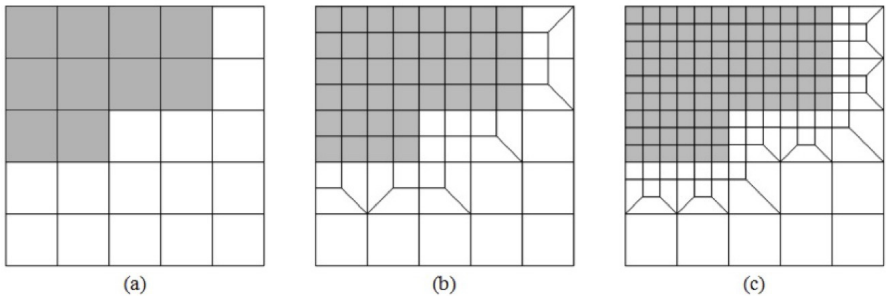


**Fig. 1.** Quadrilateral refinement with transition templates. (a) Original mesh and shaded refinement region. (b) Mesh refined with 2-refinement. (c) Mesh refined with 3-refinement.

This adaptation algorithm uses the Automated Quadrilateral Coarsening by Ring Collapse (AQCRC) algorithm recently developed by Dewey [2]. This coarsening method provides completely localized coarsening by selecting and removing rings of adjacent faces from within a specified coarsening region as shown in figure 2. One consequence of the removal of these coarsening rings is the creation of poor quality faces and quadrilateral improvement (clean-up) is a necessary step in this process. Although the AQCRC algorithm is a very effective local coarsening technique, it assumes that the coarsening rings are closed rings and does not have any provisions for coarsening of the mesh boundaries. Because of this limitation we employ the removal of dual chords [19] to coarsen the boundaries as illustrated in figure 3.

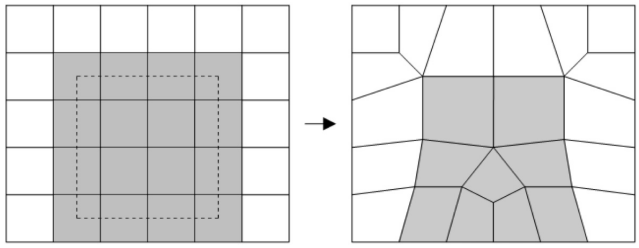

**Fig. 2.** AQCRC coarsening.

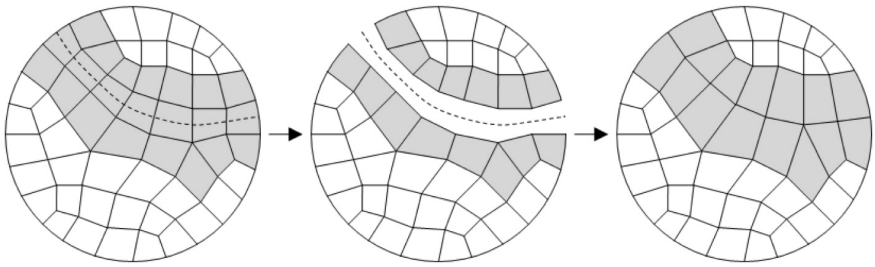

**Fig. 3.** Quadrilateral chord removal.

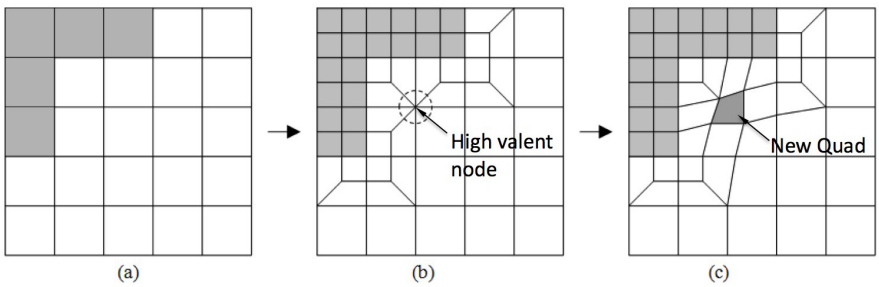


**Fig. 4.** One example of quality improvement required by refinement. (a) Shaded refinement region. (b) Seven-valence node formed from 2-refinement. (c) Mesh after quality improvement operation (face open on high-valence node).

In addition to the use of clean-up within the AQCRC algorithm, poor quality faces may form as a result of the refinement of irregular regions, making quadrilateral improvement a necessary step in this adaptation procedure. As a result, we also introduce new cleanup procedures [3], extending procedures introduced in [20], for improving the quality of an adapted mesh. For example, figure 4 shows a case where a concave refinement region forms a node with a valence of seven. This high-valence node is then removed with a face open procedure, resulting in a more structured mesh. The removal of

high valence nodes from a mesh is one of many capabilities of this quality improvement method.

### 3.3 Algorithm

The goal of this automated mesh adaptation algorithm is to modify an existing mesh so that all of the faces are as close to the size specified by a sizing function but no larger. This ensures that solution accuracy and resolution are not sacrificed for decreased computation time. The algorithm flowchart is shown in figure 5 and described by the following steps:

1. A quadrilateral mesh to be adapted and an accompanying sizing function are provided as input.
2. Each curve defining the boundary of the mesh is checked to see if coarsening is required. If a bounding curve must be coarsened, chords intersecting the boundary are removed until an appropriate size is reached.
3. If coarsening is needed anywhere in the mesh, those regions are coarsened. The clean-up algorithm is included as a step within the coarsening algorithm. If at any point, it is determined that coarsening is not needed, this step is skipped in all future iterations.
4. If refinement is needed anywhere in the mesh, those regions are refined.
5. Following the refinement of elements in the mesh, the entire mesh surface is cleaned-up.
6. Steps 3 through 5 are repeated until sufficient refinement has occurred.

### 3.4 Algorithm Example

To illustrate this algorithm, we demonstrate with the following example simulating a circular line load on a planar surface as shown in Figure 6. In this case, the area of interest is at the location of the load. For simplicity, the algorithm can be divided into three distinct parts; input, boundary coarsening, and iterative coarsening/refinement.

*Input*

This algorithm requires an already meshed surface and an appropriate sizing function to be provided as input. In this case the surface is a flat 10 x 10 plate, meshed with a perfectly structured 10 x 10 quadrilateral mesh also shown in figure 6.

The size of each quadrilateral face, $h_a$ is the average length of its four edges:

$$h_a = \frac{1}{4}\sum_{i=1}^{4} l_i \tag{1}$$

where $l_i$ is the length of the $i^{th}$ edge of the quadrilateral face. Therefore, the size of each face in this initial mesh is 1.0. The sizing function for this example specifies a very high element density with an element size of 0.1 at the location

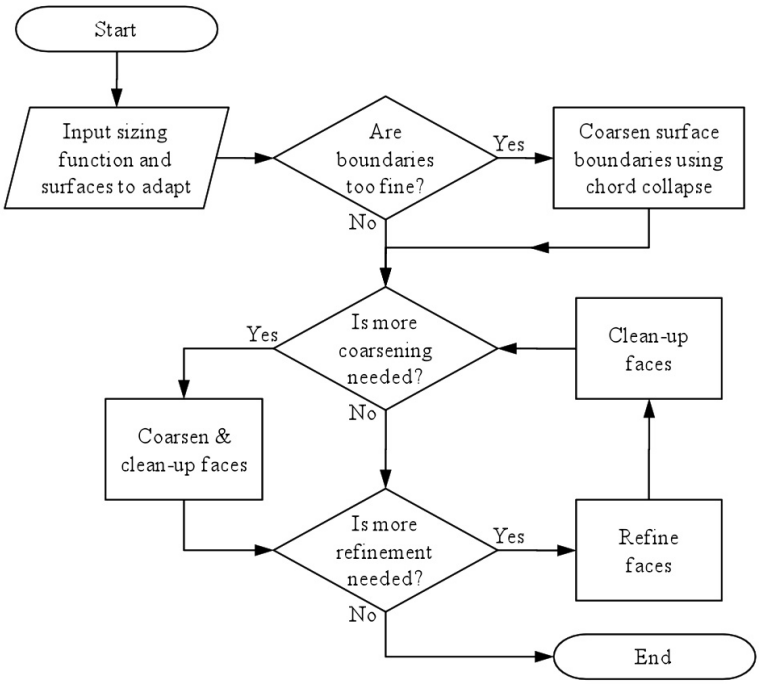


**Fig. 5.** Algorithm flowchart

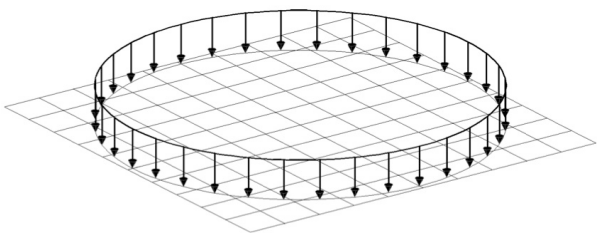

**Fig. 6.** Circular load on plane surface.

of the applied load. This specified element density gets progressively lower, varying linearly, as we move further away from the load, eventually reaching a recommended element size of nearly 5 at the center of the plate.

*Boundary Coarsening*

Since the AQCRC algorithm developed by Dewey does not allow boundary coarsening, it is achieved with simple chord removals in areas of the boundary that require larger element sizes. The edge length ratio $f_l$, defined in Equation 2, is the ratio of actual edge size $l_a$ to desired edge size $l_d$ and is calculated for all boundary edges and used to select chords for removal.

$$f_l = \frac{l_a}{l_d} \tag{2}$$

In this example, boundary coarsening is necessary near the corners of the mesh. Four chords, shown in the left panel of Figure 7 are chosen for removal. The right panel of Figure 7 shows the mesh following the removal of the four chords. To maintain a more isotropic mesh structure, each bounding curve that was coarsened is then smoothed.

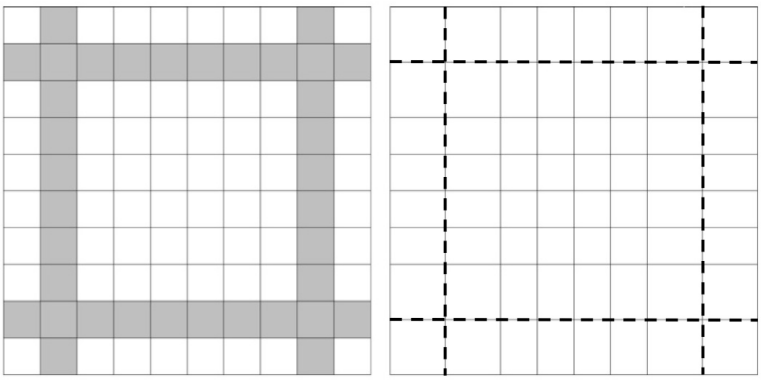

**Fig. 7.** Chords selected for removal and removed.

*Iterative Coarsening, Refining, and Quality Improvement*

The remainder of the algorithm modifies the interior of the mesh by iteratively coarsening and refining elements until the goal has been reached. To provide a balanced approach to the adaptation problem, each iteration of this algorithm alternates between coarsening and refinement. Since coarsening tends to make the mesh less structured and refinement tends to make the mesh more structured, the algorithm always begins with coarsening which is followed by refinement. Refining after coarsening also helps to achieve the goal of ensuring that the elements in the mesh are smaller than specified by the sizing function.

Each iteration begins by calculating the size ratio of each face $f_s$ as:

$$f_s = \frac{h_a}{h_d} \tag{3}$$

where $h_a$ is the actual face size as defined in Equation 1 and $h_d$ is the desired face size as specified by the sizing function. A size ratio greater than 1.0 indicates that the face is too large and should be refined; a size ratio less than 1.0 indicates that the face is too small and can be coarsened.

To better control the amount of coarsening that takes place and to ensure that the coarsening operation does not overshadow refinement requirements, a dynamic threshold $t_c$, given as:

$$t_c = 1.0 - 0.2n_c \tag{4}$$

where $n_c = 0, 1, 2, ...$ is an integer defined by the number of iterations.

Any face with a size ratio less than the coarsening threshold is considered too small and should be coarsened. For example, in the first iteration, any face with a size ratio less than 1.0 is considered for coarsening. In later iterations, the coarsening threshold is relaxed until the sixth iteration when it becomes zero and disappears. Also, if at any point in the adaptation process, fewer than 10% of the faces in the mesh require coarsening, the coarsening is considered complete and is skipped in all future iterations. This requirement helps to ensure that the same mesh regions are not being repeatedly coarsened and refined. Figure 8(a) shows the faces selected for coarsening in the example. This shaded region is coarsened and the resulting mesh topology can be seen in Figure 8(b).

Since the coarsening algorithm requires a contiguous region of quadrilateral faces to create coarsening rings, a lone face requiring coarsening surrounded by faces that do not require coarsening will automatically be neglected by the AQCRC algorithm, making sure coarsening does not extend outside of the desired region.

After the first iteration of coarsening, the size ratio is re-calculated for all of the faces in the mesh in preparation for refinement. Any face with a size ratio greater than 1.0 is considered too large and requires refinement. This limit of 1.0 is not relaxed at any time throughout the algorithm; however, a dynamic refinement threshold $t_r$, defined in Equation 5, is used to separate the elements requiring refinement into two categories.

$$t_r = 1.25 - 0.05n_r \tag{5}$$

where $n_r = 0, 1, 2, ...$ is an integer defined by the number of iterations.

Any element with a size ratio greater than 1.0 and greater than the refinement threshold is considered a high-refine face, while any face with a size ratio greater than 1.0 but less than the refinement threshold is considered a low-refine face. In the refinement step, only the high-refine faces are refined, unless there are none, in which case the low-refine faces are refined. The purpose of the separation between faces is that the low-refine faces are often very close to the high-refine faces and fall within their transition zones which are refined by means of transition template insertion. Similar to the coarsening threshold, the refinement threshold gradually shrinks the allowable range of low-refine face until the refinement threshold equals 1.0 and disappears. At this point, all faces with a size ratio greater than 1.0 are high-refine elements.

If at any time, less than 3% of the faces are considered low-refine faces and less than 0.5% of the faces are considered high-refine faces, refinement is deemed sufficient. If these criteria are met, however, future iterations of refinement are not precluded as future iterations of coarsening are.

In Figure 8(b) the high-refine faces are shaded dark gray and the low-refine faces are shaded light gray. As expected, the low-refine faces are in close

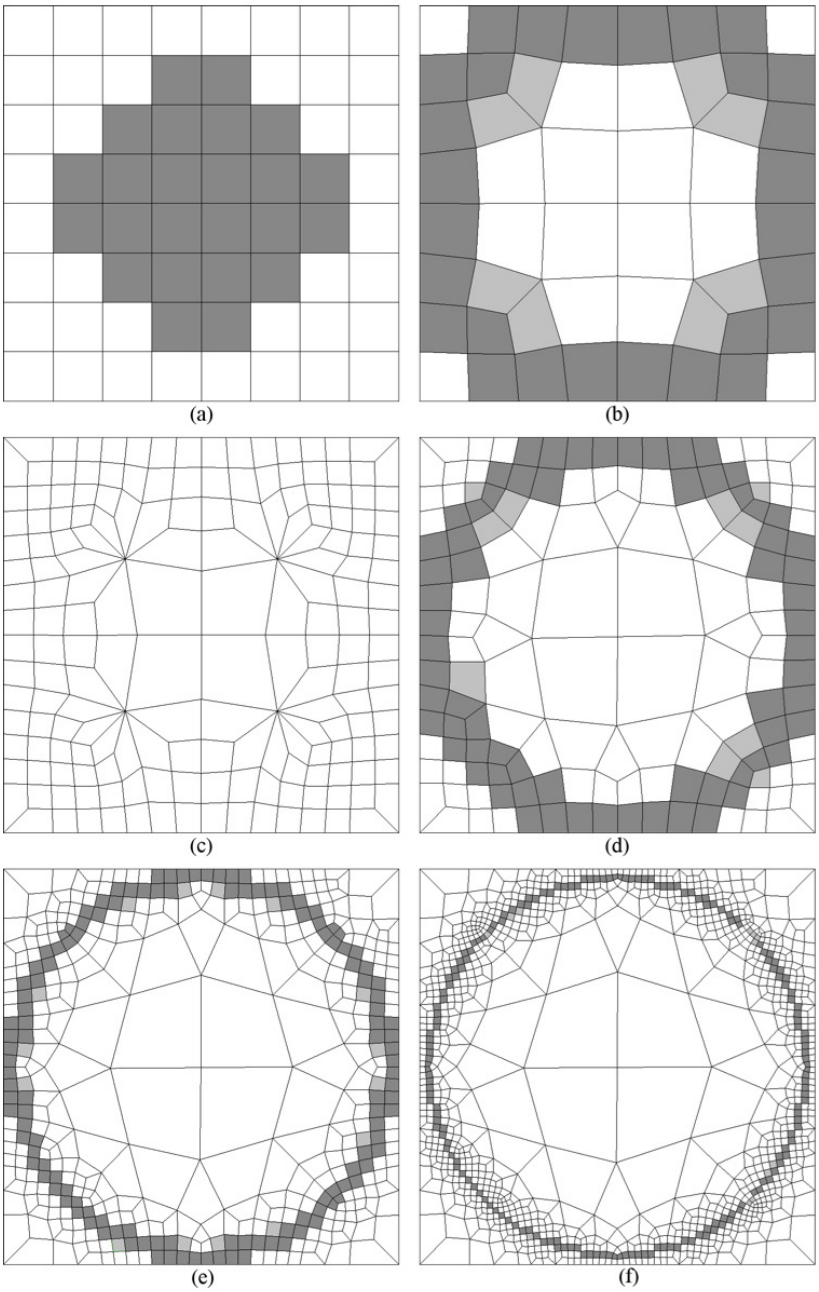


**Fig. 8.** Coarsening, refinement, and quality improvement steps. (a) Iteration 1, coarsening region. (b) Iteration 2, refinement regions. (c) Iteration 2, before quality improvement. (d) Iteration 3, refinement regions. (e) Iteration 4, refinement regions. (f) Iteration 5, refinement regions.

proximity to the high-refine faces and, in fact, fall in the transition zone. The mesh topology resulting from the refinement of the high-refine faces is shown in Figure 8(c). Note the creation of four 9-valence nodes as a result of the refinement of the irregular high-refine region. Because of situations like this, the quadrilateral improvement algorithm is applied after each instance of refinement. In the clean-up procedure, nodes with a valence greater than 6 are considered unacceptable and mesh topology is changed to remove the high valence. The new mesh topology following the clean-up algorithm is shown in Figure 8(d) where the unacceptable 9-valence nodes have been reduced to acceptable 5-valence nodes.

The algorithm then iteratively coarsens and refines the mesh until sufficient coarsening and refinement have both taken place. At this point in the example, after the first refinement step, it was determined that fewer than 10% of the faces had a size ratio that warranted coarsening; therefore, coarsening is now considered complete for all future iterations. Following this completion of coarsening, only refinement steps occur. Figures 8(d-f) show the successive refinement iterations for the remainder of this example. The final adapted mesh is shown in Figure 9.

Table 1 provides the distribution of size ratios of the faces in the final mesh. Note that nearly all of the faces have a size ratio less than 1.0 and are therefore smaller than desired. Since the goal of this adaptation is to provide elements close to the desired size, but not larger, this is a good result. It is not surprising, however, that some of the elements are too large since this

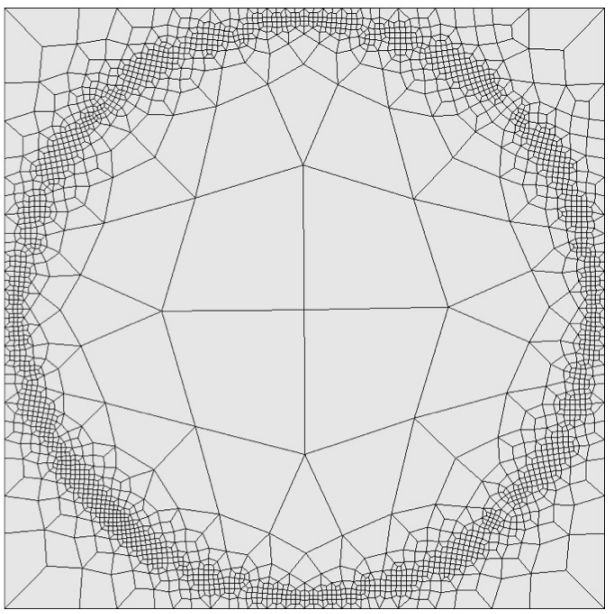

**Fig. 9.** Adapted mesh of circular load on plane surface.

**Table 1.** Results of circular load adaptation

| Size Ratio $f_s$ | Number of Faces | Percent of Total | Size Ratio $f_s$ | Number of Faces | Percent of Total |
|---|---|---|---|---|---|
| <0.5 | 1485 | 61.0% | 1.0 - 1.1 | 36 | 1.5% |
| 0.5 - 0.8 | 708 | 29.1% | 1.1 - 1.2 | 14 | 0.6% |
| 0.8 - 0.9 | 114 | 4.7% | 1.2 - 1.5 | 0 | 0.0% |
| 0.9 - 1.0 | 77 | 3.2% | >1.5 | 1 | 0.0% |
| | 2384 | 97.9% | | 51 | 2.1% |

method uses an isotropic smoothing scheme which ignores the desired size specified by the sizing function.

## 4 Examples

We show two additional examples to illustrate the results of this new quadrilateral adaptation scheme. Both of the examples show the initial mesh and a contour plot of the sizing function, as well as the mesh after adaptation and a table with data showing the results of the adaptation. The final example, a plate with a hole, also provides results from a finite element analysis of the plate under a tensile load. In each example the original mesh was created with the paving algorithm in the mesh generation software package, CUBIT [21].

In these examples, and other experiments not included here [22], the size ratio data resulting from the adaptation technique are very similar. In each case, 2% or fewer of the faces are larger than their desired size and nearly all of the larger faces are within 10% of the target. This is a promising result considering the goal is to make sure most, if not all, of the elements are smaller than the desired size. The primary reason that there are some faces that are too large is that the smoothing algorithm used as part of the clean-up operations does not take into account the sizing function and may work against the desired size.

Even though there are a few faces with a size ratio greater than 1.0, more than 80% of the elements have a size ratio of less than 0.8, suggesting that this adaptation method over-refined the meshes by adding more elements than were necessary. This over-refinement, however, is to be expected since the quadtree refinement scheme divides all faces in the refinement region into four, resulting in a reduction of interval size by half. Additionally, the transition zone around the region is refined by adding templates to ensure a conformal mesh.

### 4.1 Nosecone

The nosecone in this example is a non-planar surface with a paved quadrilateral mesh. Figure 10 shows an isotropic view the original mesh and a side view of the sizing function. The original element size in this example was 1.0

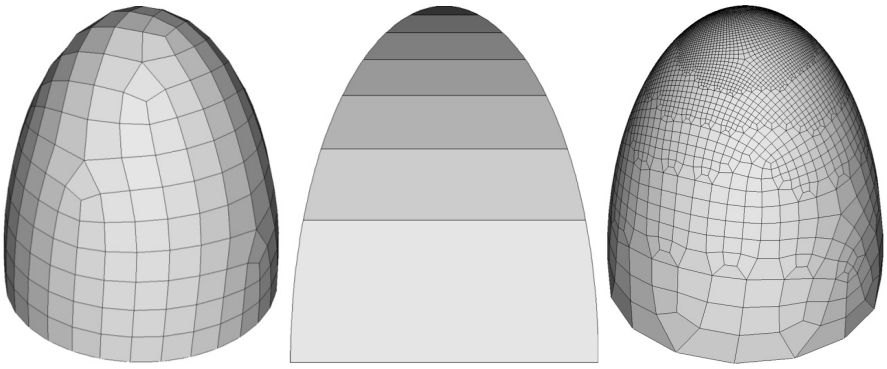

**Fig. 10.** Original mesh of nosecone (left) with contour plot of sizing function (middle) and final addapted mesh (right).

and the desired size ranged from 0.1 to 3. The sizing function used for this adaptation specified a high element density at the tip of the nosecone where the curvature is high and low element density away from the tip at the base. This example also illustrates how a sizing function might be used to adapt a mesh based on geometric characteristics of the model. In addition to the refinement near the tip of the object, note the difference in element size along the curve at the base of the nosecone.

Table 2 shows the distribution of size ratios through the mesh. In this example, fewer than 3% of the faces are too large and fewer than 7% of the faces are less than half of the desired size. This example provided very good results for not over-refining the mesh.

**Table 2.** Adaptation results of nosecone example.

| Size Ratio $f_s$ | Number of Faces | Percent of Total | Size Ratio $f_s$ | Number of Faces | Percent of Total |
|---|---|---|---|---|---|
| <0.5 | 132 | 6.5% | 1.0 - 1.1 | 50 | 2.4% |
| 0.5 - 0.8 | 1494 | 73.0% | 1.1 - 1.2 | 1 | 0.0% |
| 0.8 - 0.9 | 233 | 11.4% | 1.2 - 1.5 | 0 | 0.0% |
| 0.9 - 1.0 | 136 | 6.6% | >1.5 | 1 | 0.0% |
| | 1995 | 97.5% | | 51 | 2.5% |

### 4.2 Plate with Hole in Tension

This example models a plate with a hole under a tensile loading, as shown in Figure 11. Due to symmetry of both the geometry and loads, this problem can be reduced to an analysis of a quarter of the plate, denoted by the shaded region. The three locations, A, B, and C, have been marked on the diagram

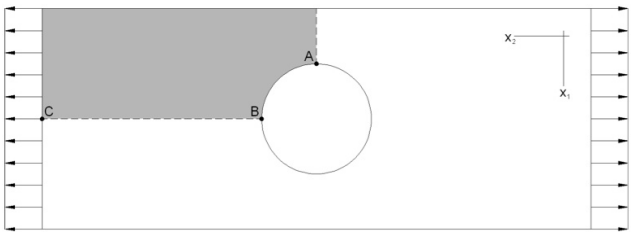


**Fig. 11.** Model of plate with hole in tension.

**Table 3.** Adaptation results of plate with hole in tension.

| Size Ratio $f_s$ | Number of Faces | Percent of Total | Size Ratio $f_s$ | Number of Faces | Percent of Total |
|---|---|---|---|---|---|
| <0.5 | 93 | 7.9% | 1.0 - 1.1 | 7 | 0.6% |
| 0.5 - 0.8 | 924 | 79.0% | 1.1 - 1.2 | 0 | 0.0% |
| 0.8 - 0.9 | 120 | 10.3% | 1.2 - 1.5 | 0 | 0.0% |
| 0.9 - 1.0 | 26 | 2.2% | >1.5 | 0 | 0.0% |
| | 1163 | 99.4% | | 7 | 0.6% |

where displacement results (see table 4) have been recorded after an analysis using the finite element program, ADINA [23].

The initial mesh of this example is shown in Figure 12 with an average element size of about 0.6. The sizing function used to adapt this mesh was based off of the stress error estimates determined from the analysis of the original mesh also shown in Figure 12. In this figure, the darker colors represent more error. The sizing function determined from this analysis specified an element size of 0.04 in the areas of highest error to an element size of 1.5 in areas with small error. The mesh resulting from the adaptation procedure is shown in Figure 13 and size ratio results of the adaptation are provided in Table 3.

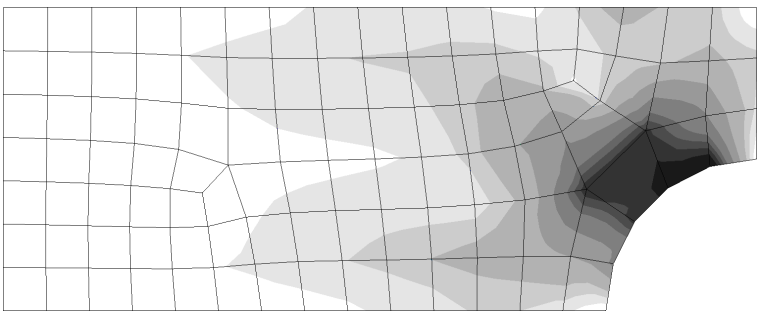

**Fig. 12.** Band plot of stress error used to define sizing function for plate with hole in tension.

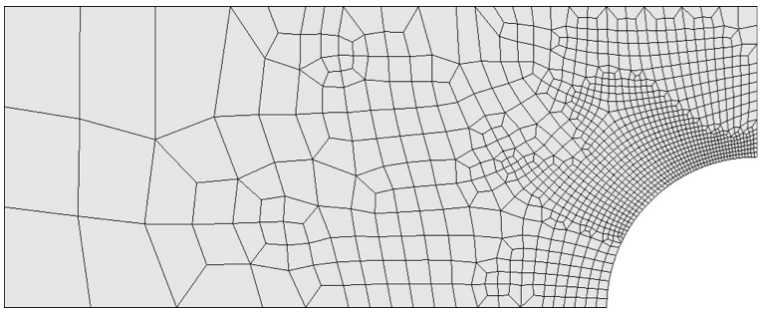

**Fig. 13.** Adapted mesh of plate with hole in tension.

**Table 4.** Results of finite element analysis.

| | Mesh Info | | Effective Stress | | Displacements | | |
|---|---|---|---|---|---|---|---|
| | Nodes | Faces | Max Value | Max Error | $\Delta x_1$ at A | $\Delta x_2$ at B | $\Delta x_2$ at C |
| Coarse | 121 | 97 | 94.3 | 32.08 | 0.00143 | 0.00279 | 0.00467 |
| Medium | 1770 | 1677 | 106.5 | 19.23 | 0.00154 | 0.00287 | 0.00474 |
| Fine | 6973 | 6788 | 107.9 | 12.33 | 0.00155 | 0.00288 | 0.00475 |
| Adapted | 1232 | 1170 | 108.3 | 7.53 | 0.00154 | 0.00287 | 0.00474 |

In addition to the initial coarse mesh and the adapted mesh, the quarter-plate was also meshed with two other meshes, each much more fine than the coarse base mesh. These meshes were used to help show convergence to a solution as well as to compare error between analyses of each of the meshes. Results shown in table 4 indicate that stress error is much more uniform across the domain in the adapted mesh than in any of the other analyzed meshes.

The maximum estimated stress error is significantly reduced by the adapted mesh. These results are significant especially when considering that the adapted mesh has only 70% of the nodes in the medium mesh and fewer than 20% of the nodes in the fine mesh. Not only does the adapted mesh provide virtually equal displacement values and superior stress values, it does so with fewer elements while reducing the estimated error. Although this is a very small problem and the time savings were negligible, the savings of computational effort on a large problem can be significant.

The results of this analysis not only show the effectiveness of this adaptation algorithm in providing an efficient solution to a computational mechanics problem, but also the importance of mesh adaptation generally in finite element problems.

## 5 Conclusion

The ability to adapt a finite element mesh is critical to providing an efficient analysis to many finite element problems. Although there are currently

effective quadrilateral adaptation techniques available, none of them are truly general in that they can modify the element density to match a sizing function by adding and removing elements without having to re-mesh all or part of the domain.

Recent developments in localized, automated quadrilateral coarsening have made it possible to combine quadrilateral refinement, coarsening, and quality improvement techniques into a conformal, all-quadrilateral adaptation method. Given a sizing function, this new adaptation technique iteratively coarsens and refines the mesh domain to provide a mesh with an element density reasonably close to that specified by the sizing function. As shown in examples, this method is an effective way to streamline the computational analysis of a finite element mesh by providing high element density in areas of the mesh that require high accuracy or geometric resolution while removing elements in less important areas of the mesh to decrease element density and save computation time.

### 5.1 Further Research

The adaptation technique described in this work effectively adds and removes elements resulting in an adapted mesh that improves accuracy or resolution where needed while improving the efficiency of the analysis by removing elements away from the area of interest. Although the results shown in this work are promising, there are still improvements that can be made and more research that can be done.

One way to improve this algorithm is to provide adaptive smoothing with refinement and coarsening. The smoothing technique currently employed in this algorithm attempts to improve the quality of the mesh by re-distributing the nodes, but does not take into account the desired element size specified by the given sizing function. In fact, the smoothing algorithm may work against the size function by attempting to create a uniformly sized mesh while the sizing function has specified a mesh with varying element density. Coupling this $h-$adaptation method with an $r-$adaptation technique that considers the element size specified by the sizing function [24] would be a major improvement to this algorithm.

In some finite element applications, particularly computational fluid dynamics problems, anisotropic elements with a high aspect ratio are desired at mesh boundaries. This adaptation technique does not account for isotropy and adds or removes elements based solely on their size. By more selectively choosing where to add elements, or even applying chord dicing capabilities, this adaptation method could be modified to allow for anisotropy.

One purpose of this research was to provide a springboard into the development of an automated all-hexahedral mesh adaptation algorithm. Recent developments have been made in conformal hexahedral refinement [1] [25] that provide localized refinement and are robust on both structured and unstructured hexahedral meshes. Additional developments have been made in automated hexahedral coarsening as well. Woodbury [26] recently introduced a

new method that provides localized conformal coarsening to an all-hexahedral mesh. Woodbury's method isolates the coarsening region through pillowing and then uses chord-collapse operations to redirect hexahedral sheets so they are located entirely within the desired coarsening region. Additionally, this method does account for boundary and surface coarsening and therefore does not have the same limitations as the AQCRC algorithm used for quadrilateral adaptation in this work. One potential difficulty in the development of an automated hexahedral adaptation scheme, however, is providing quality improvement operations to ensure a high quality mesh. The improvement operators used in quadrilateral mesh improvement do not extend directly into 3-dimensions and topological restrictions in hexahedra make local topology changes very difficult.

## References


1. Parrish, M., Borden, M., Staten, M.L., Benzley, S.E.: A Selective Approach to Conformal Refinement of Unstructured Hexahedral Finite Element Meshes. In: Proceedings of 16th International Meshing Roundtable, pp. 251–268 (2007)
2. Dewey, M.W.: Automated Quadrilateral Coarsening by Ring Collapse, Master's Thesis, Brigham Young University, Provo (2008)
3. Anderson, B.D., Shepherd, J.F., Daniels, J., Benzley, S.E.: Quadrilateral Mesh Improvement, Research Note. In: 17th International Meshing Roundtable (2008)
4. Blacker, T.D., Stephenson, M.B.: Paving: A New Approach to Automated Quadrilateral Mesh Generation. International Journal for Numerical Methods in Engineering 32(4), 811–847 (1991)
5. Quadros, W.R., Vyas, V., Brewer, M., Owen, S.J., Shimada, K.: A Computational Framework for Generating Sizing Function in Assembly Meshing. In: Proceedings of 14th International Meshing Roundtable, pp. 55–72 (2005)
6. Borouchaki, H., Frey, P.J.: Optimization Tools for Adaptive Surface Meshing, AMD Trends in Unstructured Mesh Generation. ASME 220, 81–88 (1997)
7. Borouchaki, H., Frey, P.J.: Adaptive Triangular Quadrilateral Mesh Generation. International Journal for Numerical Methods in Engineering 41, 915–934 (1998)
8. Feng, Y.T., Peric, D.: Coarse Mesh Evolution Strategies in the Galerkin Multigrid Method with Adaptive Remeshing for Geometrically Non-linear Problems. International Journal for Numerical Methods in Engineering 49, 547–571 (2000)
9. Botkin, M.E., Wang, H.P.: An Adaptive Mesh Refinement of Quadrilateral Finite Element Meshes Based upon an a posteriori Error Estimation of Quantities of Interest: Modal Response. Engineering with Computers 20, 38–44 (2004)
10. Baehmann, P.L., Shephard, M.S.: Adaptive Multiple-Level h-Refinement in Automated Finite Element Analyses. Engineering with Computers 5, 235–247 (1989)
11. Branets, L., Carey, G.F.: Smoothing and Adaptive Redistribution for Grids with Irregular Valence and Hanging Nodes. In: Proceedings of 13th International Meshing Roundtable, pp. 333–344 (2004)
12. Zhang, Y., Bajaj, C.: Adaptive and Quality Quadrilateral/Hexahedral Meshing From Volumetric Data. In: Proceedings of 13th International Meshing Roundtable, pp. 365–376 (2004)

13. Jiao, X., Colombi, A., Ni, X., Hart, J.C.: Anisotropic Mesh Adaptation for Evolving Triangulated Surfaces. In: Proceedings of 15th International Meshing Roundtable, pp. 173–190 (2006)
14. Sandhu, J.S., Menandro, F.C.M., Liebowitz, H.: Hierarchical Mesh Adaptation of 2D Quadrilateral Elements. Engineering Fracture Mechanics 50, 727–735 (1995)
15. Albuquerque, N.M.: Cubit 11.1 user documentation, Sandia National Laboratories (2009), `http://cubit.sandia.gov/documentation.html`
16. Borouchaki, H., Hecht, F., Frey, P.J.: Mesh Gradation Control. International Journal for Numerical Methods in Engineering 13, 1143–1165 (1998)
17. Persson, P.-O.: Mesh Size Functions for Implicit Geometries and PDE-based Gradient Limiting. Engineering with Computers 22(2), 95–109 (2006)
18. Schneiders, R.: Refining Quadrilateral and Hexahedral Element Meshes. Numerical Grid Generation in Computational Field Simulations 1, 679–688 (1996)
19. Staten, M.L., Benzley, S.E., Scott, M.: A Methodology for Quadrilateral Finite Element Mesh Coarsening. Engineering with Computers 24, 241–251 (2008)
20. Kinney, P.: Cleanup: Improving Quadrilateral Finite Element Meshes. In: Proceedings of 6th International Meshing Roundtable, pp. 449–461 (1997)
21. CUBIT 11.1 Geometry and Mesh Generation Toolkit, Sandia National Laboratories (2009), `http://cubit.sandia.gov`
22. Anderson, B.D.: Automated All Quadrilateral Mesh Adaptation through Refinement and Coarsening, Master's Thesis, Brigham Young University, Provo (2009)
23. ADINA-AUI 8.5.2, ADINA R & D Inc. (2008), `http://www.adina.com`
24. Hansen, G., Zardecki, A.: Unstructured Surface Mesh Adaptation Using the Laplace-Beltrami Target Metric Approach. Journal of Computational Physics 225, 165–182 (2007)
25. Harris, N.: Conformal Refinement of All-Hexahedral Finite Element Meshes, Master's Thesis, Brigham Young University, Provo (2004)
26. Woodbury, A.: Localized Coarsening of Conforming All-Hexahedral Meshes, Master's Thesis, Brigham Young University, Provo (2008)